ISSN: 2720-989X
JEEE
JOURNAL OF ENERGY AND ELECTRICAL ENGINEERING

Jellyfish Search Algorithm-Based Optimization of C-Type Passive Filters for Harmonic Mitigation

Mochamad Irlan Malik[1], Nurmela[2], Boy Ihsan[3], Nadya Glaudira[4], Mulyana[5]
[1,2,4] Department of Electrical Engineering, Faculty of Engineering, Universitas Siliwangi, Tasikmalaya, Indonesia
[3] Department of Electrical Engineering, Faculty of Engineering, Universitas Riau, Pekanbaru, Indonesia
[5] Department of Electrical Engineering, Faculty of Industrial Technology, Universitas Islam Sultan Agung, Semarang, Indonesia
[1] email: (mochamadirlanmalik@unsil.ac.id)

[*submitted*: 25-02-2026 | *review*: 11-04-2026 | *published*: 30-04-2026]

ABSTRACT: *The increasing penetration of nonlinear industrial loads significantly intensifies harmonic distortion in power systems, resulting in degraded power quality, increased power losses, and overheating in electrical equipment, as well as non-compliance with IEEE 519 standards. This study proposes a Jellyfish Search Algorithm (JSA)-based optimization framework for parameter tuning of C-Type passive filters in a medium-voltage industrial distribution system. The novelty of this work lies in the integration of a metaheuristic optimization approach with multi-harmonic constrained filter design to enhance attenuation performance beyond conventional analytical methods. Initial harmonic assessment reveals severe distortion levels, with total harmonic distortion (THD) reaching 23.55%, 18.67%, and 24.72% across phases L1–L3. A baseline analytical design employing dual C-Type filters tuned to the 3rd and 5th harmonics reduces THD to approximately 3.2%, meeting standard limits but still dominated by low-order harmonic components. To address this limitation, JSA is applied to optimally determine filter parameters by minimizing THD while preserving impedance characteristics at targeted harmonic frequencies. The optimized configuration further reduces THD to 1.99%, 1.66%, and 1.63% for phases L1–L3, respectively, without introducing adverse resonance effects within the studied frequency range. Convergence analysis indicates stable optimization behavior with a well-balanced exploration–exploitation mechanism. These results demonstrate that the proposed JSA-based approach provides a systematic and effective strategy for enhancing harmonic mitigation performance and advancing passive filter design in industrial power systems.*

KEYWORDS: *Jellyfish Search Algorithm, C-Type Passive Filter, Harmonic Mitigation, Total Harmonic Distortion, Individual Harmonic Distortion, Industry*

I. INTRODUCTION

The increasing penetration of nonlinear loads, power electronic converters, renewable energy systems, and electric vehicle (EV) charging infrastructures has significantly intensified harmonic distortion in modern power networks. Elevated harmonic levels deteriorate power quality, accelerate equipment aging, increase thermal losses, and may trigger malfunction in sensitive industrial systems. Recent studies have highlighted harmonic mitigation as a critical challenge in distributed and hybrid energy environments, particularly in renewable-integrated and EV-dominated grids [1], [2], [3]. Although active power filters provide dynamic compensation capability, their implementation is often associated with higher cost, complex control strategies, and maintenance requirements. Consequently, passive filtering solutions remain attractive due to their simplicity, robustness, and cost-effectiveness [4], [5], [2].

Among passive filter topologies, the C-Type passive filter has received growing attention because of its ability to suppress low-order harmonics while maintaining low fundamental frequency losses compared to conventional single-tuned and high-pass filters. Its structural configuration allows improved reactive power compensation and reduced damping losses, making it suitable for industrial and transportation applications [6]. Several studies have investigated the performance of C-Type filters and their hybrid configurations for harmonic mitigation in industrial systems [7], [8]. However, the harmonic suppression capability of C-Type filters is highly sensitive to parameter selection, including resistance, inductance, and capacitance values. Inaccurate tuning may lead to parallel or series resonance phenomena, insufficient harmonic attenuation, and undesirable reactive power injection.

To overcome parameter tuning challenges, metaheuristic optimization techniques have been increasingly adopted in passive filter design. Particle Swarm Optimization (PSO) has been utilized for optimal sizing of single-tuned filters in industrial systems [9], while Whale Optimization Algorithm (WOA) and Genetic Algorithms (GA) have demonstrated improved placement and sizing strategies for harmonic mitigation [10], [11]. Grey Wolf Optimization (GWO) and its adaptive variants have also shown promising convergence characteristics in power system applications [5], [12], [13]. More recently, data-driven and machine learning approaches have been

explored to evaluate passive filter performance under variable operating conditions [14], [15]. Despite these advancements, many optimization methods still encounter limitations such as premature convergence, insufficient balance between exploration and exploitation phases, or reduced robustness when applied to multi-harmonic industrial environments.

The Jellyfish Search Algorithm (JSA), a bio-inspired metaheuristic derived from the collective foraging behavior of jellyfish influenced by ocean currents, has recently attracted significant attention due to its adaptive time-control mechanism and superior global exploration capability [16], [17]. Advanced variants incorporating orthogonal learning strategies have further enhanced convergence accuracy and population diversity preservation [18]. JSA has demonstrated competitive performance in diverse engineering optimization problems, including energy forecasting and parameter tuning applications [19], and has shown promising potential in passive filter sizing tasks [20], [21], [22]. Despite these advantages, existing applications of JSA remain largely confined to simplified optimization scenarios and do not adequately capture the complex interactions of multi-harmonic impedance characteristics and resonance constraints inherent in practical power systems. In particular, the application of JSA to the optimal design of C-Type passive filters has not been systematically explored, especially for simultaneous multi-harmonic optimization problems. This limitation reveals a critical research gap in developing a robust and physically consistent optimization framework for real-world harmonic mitigation.

In particular, the harmonic impedance characteristics of C-Type filters across multiple frequency orders have not been systematically integrated into a robust JSA-based optimization framework. Accordingly, this study proposes a Jellyfish Search Algorithm-driven optimization model for determining the optimal R, L, and C parameters of a C-Type passive filter aimed at minimizing total harmonic distortion (THD) while ensuring stable harmonic attenuation and preventing undesirable resonance phenomena. By coupling detailed harmonic impedance modeling with an adaptive JSA optimization strategy tailored for multi-harmonic industrial environments, this work advances the current state of the art in intelligent passive filter design for modern power systems. The main contribution of this study lies in the development of an integrated multi-harmonic optimization framework that simultaneously considers impedance characteristics, resonance constraints, and adaptive parameter tuning, resulting in improved suppression of dominant harmonics and enhanced robustness compared to conventional and existing metaheuristic-based approaches.

II. METHODS

A. RESEARCH METHODOLOGY

Fig 1. illustrates the overall optimization framework for determining the optimal parameters of the C-Type passive filter using the Jellyfish Search Algorithm (JSA). The procedure begins with the input of system specifications, including fundamental frequency, harmonic orders to be mitigated, reactive power requirements, and network parameters. Based on these specifications, preliminary analytical relations of the C-Type filter are derived to establish feasible ranges for R, L, C_1, and C_2. These pre-calculated constraints ensure that the candidate solutions generated during the optimization process remain physically meaningful and electrically realizable.

Subsequently, an initial population of jellyfish is generated, where each individual represents a candidate solution. The fitness of each candidate is then evaluated based on the defined objective function, typically formulated to minimize total harmonic distortion (THD), impedance deviation at the tuned frequency, or power loss. The global best solution is identified, and the iterative process begins. At each iteration, a time control function $c(t)$governs the transition between exploration and exploitation phases. If $rand < c(t)$, the jellyfish performs passive motion (ocean current movement); otherwise, active motion (movement within swarm) is executed. Boundary checking is applied to maintain feasibility within predefined parameter limits.

After position updating, the new fitness values are computed. If a candidate solution improves its previous fitness, the position is updated; otherwise, the previous solution is retained. The global best is then revised accordingly. This process repeats until the maximum number of iterations is reached. The final global best solution represents the optimal parameter configuration of the C-Type filter, referred to as the *jellyfish bloom* state. This structured procedure ensures a balanced exploration–exploitation mechanism while maintaining electrical design constraints throughout the optimization process.

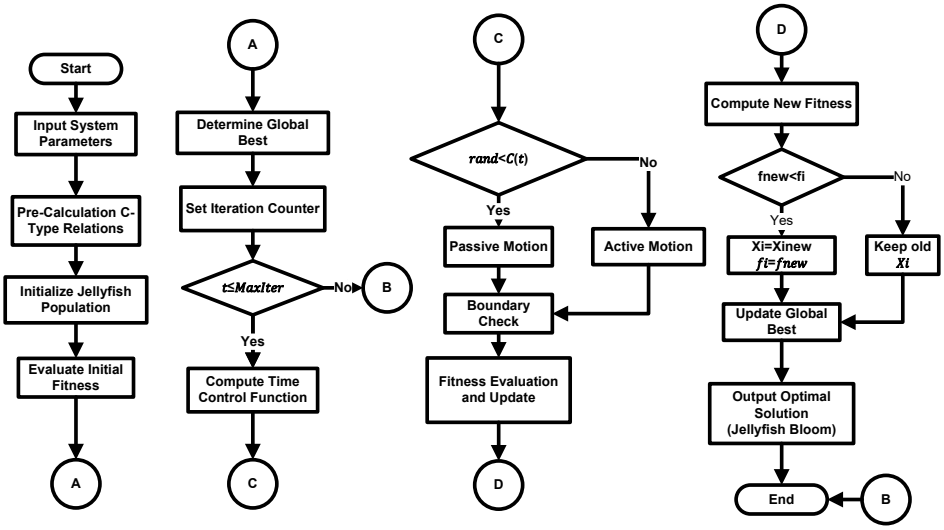

Fig 1. Flowchart of the Proposed Jellyfish Search Algorithm (JSA).

B. MEASURED CURRENT HARMONIC CHARACTERISTICS

Tbl 1. summarizes the measured current harmonic distortion obtained using a Power Quality Analyzer (PQA) at the 380 V secondary side of an 800 kVA distribution transformer operating at 50 Hz. The harmonic assessment is conducted in accordance with the limits specified in IEEE 519-2022 for low-voltage systems (≤ 1 kV). The results indicate that the 3rd harmonic (150 Hz) is the most dominant component in all phases, reaching 20.9% (L1), 16.3% (L2), and 22.0% (L3), significantly exceeding the 5% allowable limit. In three-phase four-wire systems, elevated triplen harmonics are particularly critical because they accumulate in the neutral conductor, potentially leading to excessive neutral current, overheating, and increased transformer losses.

Tbl 1. Measured Current Harmonic Distortion

Order	Freq. (Hz)	IEEE 519 Limit (%)	L1	L2	L3	Status
			(%)			
3	150	7	20.9	16.3	22.0	Exceeds
5	250	7	10.1	8.4	10.6	Exceeds
7	350	7	2.8	2.5	2.9	Within
9	450	7	2.8	2.5	2.5	Within
11	550	3.5	0	0	0	Within
THD	—	**8**	**23.55**	**18.67**	**24.72**	**Exceeds**

The 5th harmonic (250 Hz) also surpasses the permissible threshold across all phases, with magnitudes of 10.1%, 8.4%, and 10.6% for L1, L2, and L3, respectively. Such distortion levels are typically associated with nonlinear loads, including rectifiers, variable speed drives (VSDs), and other power electronic converters connected to the secondary network. Although the 7th and 9th components remain within the 5% limit and the 11th component is negligible, the Total Harmonic Distortion (THD) values—23.55% (L1), 18.67% (L2), and 24.72% (L3)—substantially exceed the 8% standard requirement, indicating non-compliance with IEEE 519-2022.

Fig 2. shows three-phase current waveforms that deviate from ideal sinusoidal shapes, indicating distortion due to dominant low-order harmonics, mainly the 3rd and 5th components. Although the 120° phase displacement is still maintained, the distortion level varies between phases, suggesting unequal harmonic loading in the system. In industry, the 3rd harmonic is mainly generated by single-phase nonlinear loads such as switched-mode power supplies and lighting systems, where triplen harmonics accumulate in the neutral conductor. The 5th harmonic, produced by three-phase devices such as VSDs and rectifiers, generates negative-sequence currents that increase losses and heating in rotating machines.

Fig 3. presents the harmonic spectrum up to the 11th order, where the 3rd harmonic is the most dominant, followed by the 5th, while higher-order components are relatively small. This confirms the waveform distortion observed in Fig 2. and shows that low-order harmonics are the main source of distortion. The unequal harmonic magnitudes between phases indicate the presence of nonlinear and partially unbalanced loads at the transformer secondary. The increase in 3rd and 5th harmonic levels reflects typical industrial load characteristics dominated by single-phase nonlinear devices and three-phase converters, highlighting the need for targeted mitigation at these orders.

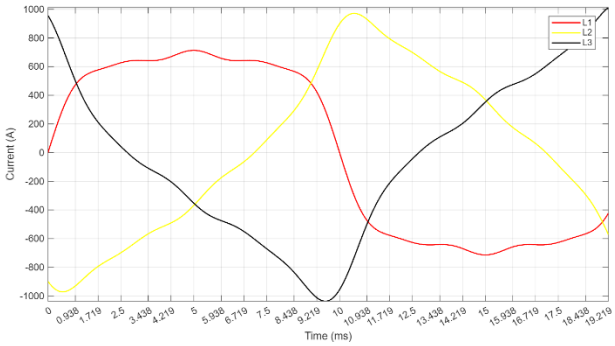

Fig 2. Measured Three-Phase Distorted Current Waveform

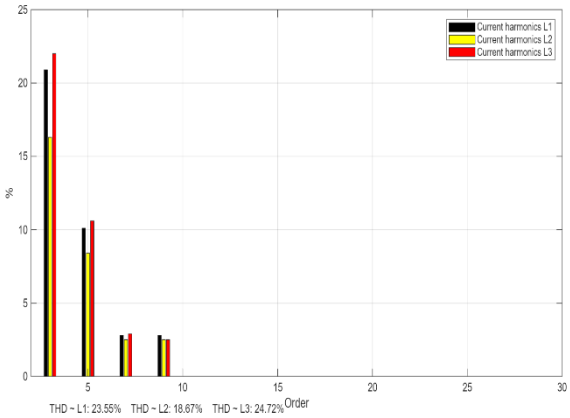

Fig 3. Current Harmonic Measurement Results

C. C-TYPE PASSIVE FILTER DESIGN

The design of a C-Type passive filter is primarily intended to mitigate low-order harmonic distortion—particularly the 3rd or 5th harmonic—while simultaneously providing reactive power compensation to improve the system power factor. Unlike a conventional single-tuned filter, the C-Type configuration incorporates an auxiliary capacitor branch to minimize fundamental frequency losses and reduce damping resistor power dissipation. The following formulation outlines the systematic design procedure [23], [24].

The first step is the determination of the required reactive power compensation [7], [25]. The reactive power supplied by the filter, Q_f, is calculated based on the desired power factor improvement using:

$$Q_f = P\ (tan\varphi_1 - tan\varphi_2) \quad (1)$$

where Prepresents the active power of the load, tan $\varphi_1$corresponds to the initial power factor condition, and tan $\varphi_2$denotes the target condition after correction. This expression quantifies the reactive power that must be injected by the filter to achieve the specified displacement power factor.

Once Q_f is determined, the main capacitor $C_1$is calculated to supply the required reactive power at the fundamental frequency. The capacitance value is obtained from:

$$C_1 = \frac{Q_f}{\omega_1 V_s^2} \quad (2)$$

where $\omega_1 = 2\pi f$ is the fundamental angular frequency and V_s is the RMS system voltage. The capacitor C_1 provides the required reactive power at the fundamental frequency and defines the primary capacitive behavior of the filter at 50 Hz.

However, unlike a conventional single-tuned filter, the C-Type configuration incorporates an auxiliary capacitor C_2, calculated as:

$$C_2 = (h_0^2 - 1)C_1 \quad (3)$$

This additional branch ensures that, at the fundamental frequency, the inductive and capacitive reactances cancel each other, thereby minimizing fundamental current flow through the damping resistor. As a result, power losses at 50 Hz are significantly reduced compared to a single-tuned configuration. The inductor value L is derived to satisfy the tuning condition at the selected harmonic frequency. One formulation is:

$$L = \frac{V_s^2}{(h_0^2 - 1)\omega_1 Q_f} \quad (4)$$

The damping resistor R controls the filter quality factor Q_{filter} and prevents excessive resonance amplification. It is expressed as:

$$\mathrm{R} = \frac{\mathrm{Q_{Filter}} V_s^2}{\mathrm{h_0} Q_f} \quad (5)$$

where Q_{filter} typically ranges from 5 to 100 depending on the desired bandwidth and damping characteristics. Lower values provide stronger damping but increase losses, whereas higher values yield sharper tuning with narrower bandwidth.

Fig 4. illustrates the configuration and operational principle of the proposed C-Type filter connected in shunt at the load bus on the secondary side of the transformer. The filter is designed to mitigate dominant harmonic currents generated by nonlinear loads while simultaneously providing reactive power compensation. Structurally, it consists of a main capacitor C_1connected in series with a parallel branch composed of an inductor L, an auxiliary capacitor C_2, and a damping resistor R. The tuning condition is achieved when the series resonance between $L$and C_2 occurs at the targeted harmonic frequency, thereby creating a low-impedance path that effectively diverts harmonic currents away from the grid. At the fundamental frequency, the impedance of the L–

C_2 branch becomes significantly high, which bypasses the damping resistor and minimizes active power losses compared to conventional single-tuned filters. The main capacitor C_1 supplies the required reactive power to support the system voltage, while the resistor R provides adequate damping to suppress resonance amplification and improve filtering stability. This configuration ensures an optimal balance between harmonic attenuation performance, reactive power compensation, and loss reduction in power systems with nonlinear loads.

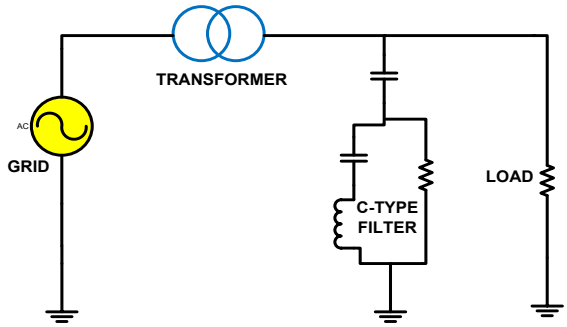

Fig 4. Design of C-Type Filter

D. OPTIMIZATION DESIGN WITH JSA

Jellyfish Search Algorithm (JSA) is a population-based metaheuristic optimization technique inspired by the natural movement of jellyfish in the ocean ecosystem [16]. As illustrated in Fig 5., the algorithm models three main behavioral mechanisms: ocean current movement, swarm interaction, and passive motion. The ocean current represents the global environmental force that guides jellyfish toward nutrient-rich regions, which in optimization corresponds to movement toward promising global solutions [26]. Swarm behavior represents interaction among individuals, allowing information exchange between candidate solutions [27]. Passive motion models random drifting within a local region, which enhances solution diversity [28]. A time control mechanism regulates the transition between these movement strategies to balance global exploration and local exploitation throughout the optimization process [17], [29]. In this study, the JSA is employed to minimize the Total Harmonic Distortion (THD) of the system in accordance with the IEEE 519 by optimizing the C-Type filter parameters at the 3rd and 5th harmonic orders.

The Jellyfish Search Algorithm (JSA) is employed in this study to optimize the parameters of dual C-Type harmonic filters tuned at the 3rd and 5th harmonic frequencies. Each jellyfish represents a candidate solution defined by an eight-dimensional decision vector as:

$$X = [C_{1,3}, L_3, C_{2,3}, R_3, C_{1,5}, L_5, C_{2,5}, R_5] \quad (6)$$

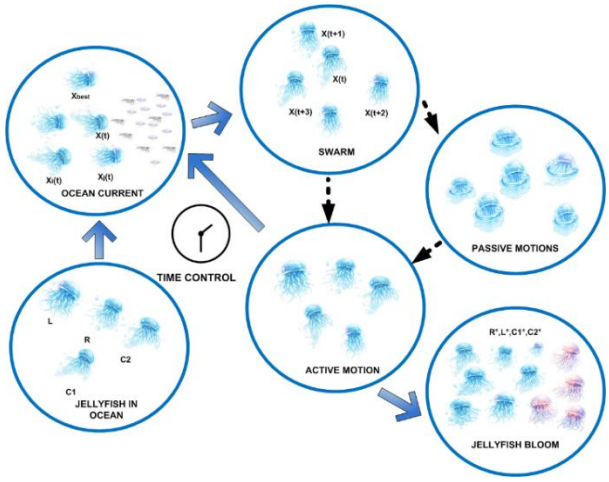

Fig 5. Mechanism of Jellyfish Search Algorithm (JSA)

where each variable corresponds directly to the physical components of the filters. This formulation ensures that the optimization process is fully consistent with the implemented MATLAB model. The initial population of jellyfish is randomly generated within predefined lower and upper bounds using a uniform distribution:

$$X_i^0 = X_{min} + rand.(X_{max} - X_{min}) \quad (7)$$

Where $i = 1,2,\dots,N$, and N=40 is the population size. The lower and upper bounds of each variable are explicitly defined based on practical design considerations of C-Type filters to ensure physically realizable component values. These limits prevent unrealistic capacitance, inductance, and resistance values while maintaining feasible resonance tuning at the target harmonic frequencies.

To control the balance between global exploration and local exploitation, a time-varying control parameter is defined as:

$$c = \left(1 - \frac{iter}{iter_{max}}\right)(2rand\ () - 1) \quad (8)$$

where t is the current iteration and T=1000 is the maximum number of iterations. The inclusion of the absolute operator ensures a non-negative control parameter, which improves convergence stability and prevents oscillatory behavior during the later stages of optimization.

The position of each jellyfish is updated using two probabilistic movement strategies. The first is the ocean current movement, which directs the solution toward the global best position:

$$X_i^{k+1} = X_i^k + 0.8r(X_{Best} - cX_i^k) \quad (9)$$

where X_{best} is the best solution obtained so far and 0.8 is the movement coefficient used in this implementation. Otherwise, a randomly selected jellyfish j is used to update the position as:

$$X_i^{k+1} = X_i^k + 0.8.rand().(X_j^k - X_i^k) \quad (10)$$

where j is a randomly selected jellyfish. The coefficient 0.8 is introduced as a step-size scaling factor to regulate movement amplitude. This value is selected empirically to balance convergence speed and stability, particularly for sensitive electrical parameters such as inductance and capacitance. Passive motion is implicitly incorporated through the stochastic nature of the update equations, where random coefficients introduce local perturbations that enhance exploration. Active motion is represented by directed movements toward better solutions, either globally through X_{best} or locally via swarm interaction, ensuring continuous improvement in solution quality.

To ensure feasibility, a boundary clipping mechanism is applied after each update to enforce the predefined lower and upper limits of the search space:

$$X_i^{t+1} = \max(X_i^{t+1}, X_{\min}) \quad (11)$$

$$X_i^{t+1} = \min(X_i^{t+1}, X_{\max}) \quad (12)$$

This approach guarantees that all candidate solutions remain within physically acceptable limits without introducing additional penalty parameters.

A greedy selection mechanism is adopted, where a new solution replaces the current one only if it yields a better fitness value. The global best solution is updated iteratively as:

$$X_{Best} = arg\ minf(X_i) \quad (13)$$

The algorithm is executed for 1000 iterations, ensuring sufficient convergence of the solution. Through iterative evaluation, adaptive position updating, and constraint enforcement, the JSA converges toward an optimal set of filter parameters that satisfies harmonic mitigation requirements, reactive power compensation, and damping constraints in a computationally efficient manner.

III. RESULTS AND DISCUSSION

The modeled system represents a medium-voltage industrial distribution network supplied from the utility grid through step-down transformers connected to the main panel. The transformer, rated in the 800 kVA class, feeds multiple three-phase feeders supplying production loads. A monitoring unit is integrated to measure RMS voltage, current, and total harmonic distortion (THD), enabling comprehensive evaluation of power quality within the facility. The analysis emphasizes harmonic propagation along the main bus due to nonlinear industrial loads.

To mitigate harmonic distortion, two C-Type passive filters tuned to the 3rd and 5th harmonic orders are installed at the main busbar. These filters are designed to provide reactive power compensation while reducing harmonic impedance at the targeted frequencies. The nonlinear loads, primarily Variable Speed Drives (VSDs), inject harmonic currents into the system, and their impact is assessed through detailed harmonic spectrum analysis to verify compliance with IEEE 519 power quality limits (see Fig 6.).

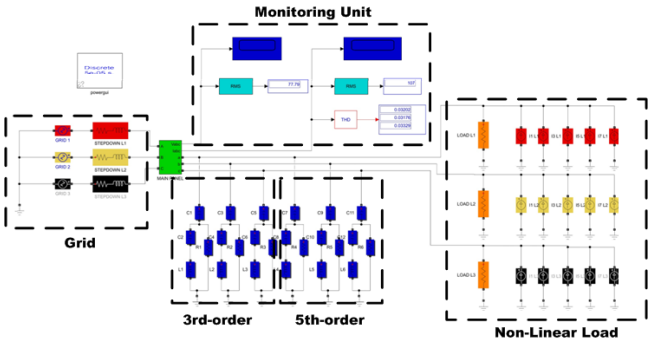

Fig 6. Industrial Harmonic Simulation Model

A. CONVENTIONAL C-TYPE FILTER DESIGN & SIMULATION

The C-Type passive filter parameters presented in Tbl 2. were obtained using conventional analytical formulations based on harmonic tuning principles. The design procedure involved determining the required reactive power compensation and tuning frequency for the targeted harmonic orders, namely the 3rd (150 Hz) and 5th (250 Hz). The calculated capacitance, inductance, and damping resistance values were adjusted per phase (L1–L3) to accommodate phase-dependent harmonic variations. For the 3rd-order filter, the inductance values range from 0.070 mH to 0.087 mH, while the damping resistance varies between 2.955 Ω and 4.562 Ω. The secondary capacitor C_2 maintained within the range of 11.640–14.420 mF to ensure effective attenuation at 150 Hz. In contrast, the 5th-order filter requires smaller inductance values (approximately 0.023–0.029 mH) and significantly lower damping resistance. This reduction reflects the higher tuning frequency and corresponding impedance characteristics at 250 Hz. Moreover, the increase in C_2 to 34.920–43.250 mF indicates a higher reactive component necessary to properly shape the frequency response at the targeted harmonic.

Tbl 2. C-Type Filter Parameters Calculated by Conventional Method

Phase	Order	C_1(mF)	C_2(mF)	L(mH)	R(Ω)
L1	3rd	1.802	14.420	0.070	2.955
L2	3rd	1.455	11.640	0.087	4.562
L3	3rd	1.655	13.240	0.076	3.990
L1	5th	1.802	43.250	0.023	0.301
L2	5th	1.455	34.920	0.029	0.719
L3	5th	1.655	39.720	0.025	0.551

Following parameter calculation, the filter models were implemented in the MATLAB/Simulink environment and integrated into a three-phase power system supplying nonlinear loads. The harmonic spectrum was evaluated using Fast Fourier Transform (FFT) analysis to determine the Individual Harmonic Distortion (IHDi) and Total Harmonic Distortion (THD). The results are summarized in Tbl 3. and illustrated in Fig 7. As observed in Tbl 3. the conventional C-Type filter effectively attenuates the dominant harmonic components, with the 3rd-order distortion reduced to the range of 3.09–3.31%, significantly below the allowable limits defined by IEEE 519. Similarly, the 5th harmonic is suppressed to below 0.65%, while higher-order components (7th, 9th, and 11th) are reduced to negligible levels. This indicates that the filter provides low impedance paths at the targeted harmonic frequencies, thereby diverting harmonic currents away from the main system. The resulting THD values of 3.25%, 3.16%, and 3.36% for phases L1, L2, and L3, respectively, further confirm that the system operates well within the prescribed limit. However, it is evident that the 3rd harmonic remains the dominant component across all phases. This suggests that although the analytical design method ensures compliance, the tuning condition does not fully align with the actual harmonic characteristics of the system.

Tbl 3. Simulated IHDi Results Using the Conventional Filter Design

Order	Freq. (Hz)	IEEE 519 Limit (%)	L1	L2	L3	Status
			(%)			
3	150	7	3.20	3.09	3.31	Within
5	250	7	0.60	0.64	0.62	Within
7	350	7	0.07	0.07	0.07	Within
9	450	7	0.01	0.01	0.01	Within
11	550	3.5	0	0	0	Within
THD	—	**8**	**3.25**	**3.16**	**3.36**	**Within**

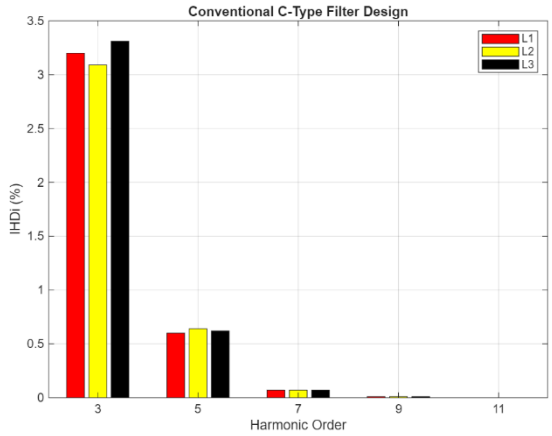

Fig 7. IHDi Spectrum by Conventional Methods

Nevertheless, although the system satisfies the standard requirements, the 3rd harmonic remains the dominant distortion component across all phases. This indicates that while the analytical method ensures acceptable performance, the parameter set may not represent a globally optimal solution. Therefore, further refinement using metaheuristic optimization (JSA) is proposed to enhance harmonic suppression and improve overall system performance.

B. JSA-BASED C-TYPE FILTER DESIGN & SIMULATION

Fig 8. illustrates the convergence characteristics of the Jellyfish Search Algorithm (JSA) for each phase (L1, L2, and L3) over 1000 iterations. The fitness trajectories exhibit a rapid initial decrease followed by gradual stabilization, indicating efficient global exploration in the early stages and effective local exploitation as the algorithm approaches convergence. The absence of oscillatory divergence or premature stagnation suggests that the search dynamics are well-balanced, ensuring numerical stability and consistent convergence behavior.

From a physical perspective, the convergence behavior reflects the algorithm's capability to iteratively adjust the C-Type filter parameters—capacitance, inductance, and damping resistance—toward an optimal impedance profile at the targeted harmonic frequencies. During the early iterations, large fitness reductions indicate that the algorithm rapidly identifies parameter regions that significantly reduce harmonic distortion by improving impedance matching at dominant harmonic components. As the iteration progresses, the refinement phase fine-tunes the parameter values, leading to more precise harmonic attenuation without overcompensation.

For phase L1, the significant fitness reduction observed between iterations 50 and 400 indicates that the algorithm quickly locates a near-optimal parameter region, followed by minor adjustments that enhance solution accuracy. In phase L2, the delayed but sharp decrease around iteration 100 suggests a broader initial exploration, allowing the algorithm to avoid local minima before converging steadily toward an optimal solution. Similarly, phase L3 exhibits a stepwise convergence pattern, reflecting gradual improvements in parameter coordination, particularly in balancing reactive components and damping effects. These convergence patterns demonstrate that JSA effectively optimizes the interaction among filter components, ensuring that the resulting parameter set not only minimizes harmonic distortion but also maintains stable system behavior. Consequently, the algorithm is capable of identifying a well-coordinated combination of C-Type filter parameters that improves harmonic

mitigation performance while avoiding suboptimal tuning conditions typically associated with conventional design methods. These convergence patterns demonstrate that JSA effectively optimizes the interaction among filter components, ensuring that the resulting parameter set not only minimizes harmonic distortion but also maintains stable system behavior.

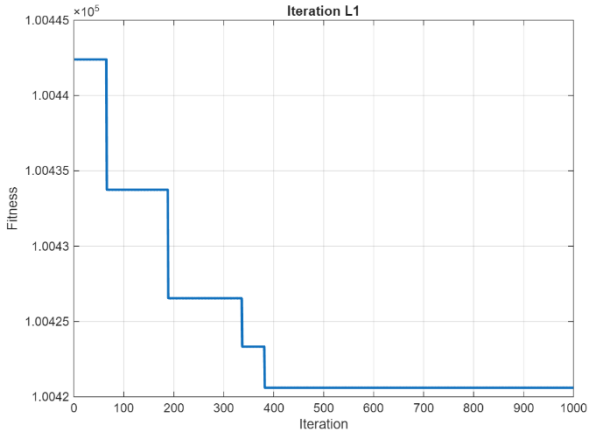

(a)

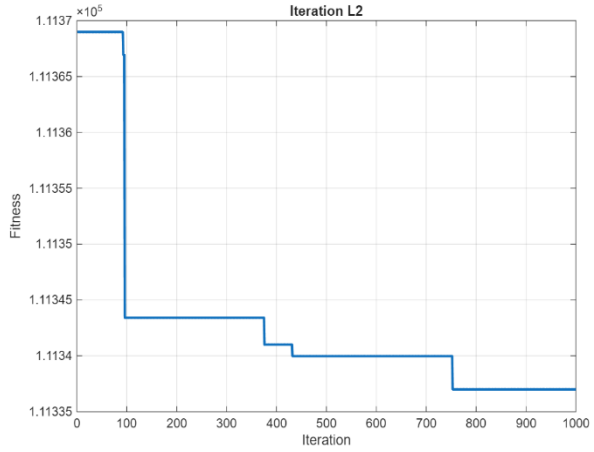

(b)

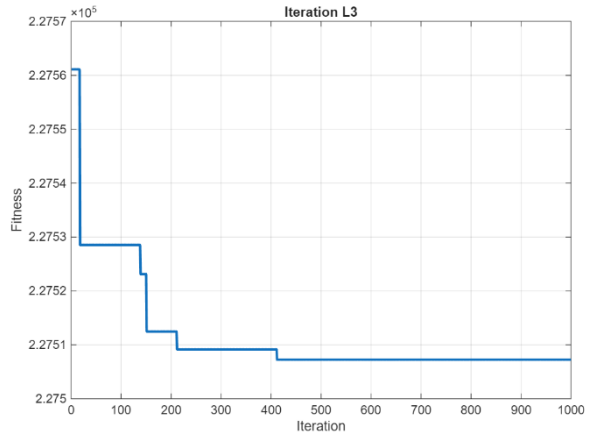

(c)

Fig 8. Iteration Test Results on Phases L1, L2, and L3

Tbl 4. presents the optimized design parameters of the C-Type passive filter for the 3rd and 5th harmonic orders in each phase. For the 3rd harmonic (150 Hz), the optimized capacitance C_1 ranges from 2.513 to 2.929 mF, while C_2 varies between 16.812 and 25.235 mF. The inductance L remains relatively small (0.055–0.138 mH), ensuring accurate resonance tuning at the targeted harmonic frequency. The damping resistance R lies between 3.354 and 4.590 Ω, providing sufficient attenuation while controlling the quality factor to prevent excessive resonance amplification.

For the 5th harmonic (250 Hz), a substantial increase in C_2 (39.101–50.497 mF) is observed, accompanied by significantly lower damping resistance values (0.504–0.751 Ω). This configuration is consistent with the inherent characteristics of the C-Type filter topology, where the damping branch minimizes fundamental-frequency losses while effectively suppressing higher-order harmonics. The variation of parameters across phases indicates that JSA adaptively adjusts the filter components according to phase-specific load characteristics, leading to individually optimized solutions rather than uniform parameter allocation.

Tbl 4. C-Type Filter Component Values Optimized by JSA

Phase	Order	C_1 (mF)	C_2 (mF)	L (mH)	R (Ω)
L1	3rd	2.929	25.235	0.055	3.354
L2	3rd	2.690	16.812	0.138	4.590
L3	3rd	2.513	18.702	0.108	4.224
L1	5th	2.062	50.497	0.052	0.504
L2	5th	1.490	39.101	0.154	0.751
L3	5th	2.567	46.871	0.106	0.555

Tbl 5. and Fig 9. present the Individual Harmonic Distortion (IHDi) spectrum after applying the optimized filter parameters obtained through JSA. For the 3rd harmonic (150 Hz), IHDi values are reduced to 1.96% (L1), 1.66% (L2), and 1.62% (L3), all significantly below the IEEE limit of 7%. At the 5th harmonic (250 Hz), IHDi decreases further to 0.32%, 0.13%, and 0.18% for L1, L2, and L3, respectively. The 7th and 9th harmonics exhibit negligible distortion levels below 0.06%, while the 11th harmonic component is effectively eliminated (0%). These results demonstrate strong attenuation performance across both targeted and non-targeted harmonic orders.

The Total Harmonic Distortion (THD) values are 1.99% (L1), 1.66% (L2), and 1.63% (L3), all well below the IEEE 519 limit of 8%. Although the harmonic spectrum remains dominated by the 3rd harmonic component, its magnitude is significantly reduced compared to the conventional design. This improvement is attributed to the optimized tuning of the filter parameters, which minimizes the equivalent impedance at dominant harmonic frequencies. The

coordinated adjustment of inductance and capacitance shifts the resonance condition closer to the actual harmonic spectrum, thereby enhancing harmonic current absorption. In addition, the increased capacitance (particularly C_2) contributes to shaping the frequency response and provides a broader attenuation bandwidth. The absence of harmonic amplification at non-targeted frequencies (7th–11th orders) indicates that no significant parallel resonance is excited, suggesting that no additional impedance peaks are introduced into the system. The damping resistance further reduces the quality factor, preventing sharp resonance behavior and mitigating instability risks. Compared to the conventional approach, the JSA-based optimization achieves a more accurate alignment between filter tuning and the system's harmonic profile through its global–local search mechanism. As a result, the optimized design not only satisfies IEEE 519 requirements but also provides improved robustness and more consistent harmonic mitigation performance.

Tbl 5. Simulated IHDi Results After JSA-Based Optimization

Order	Freq. (Hz)	IEEE 519 Limit (%)	L1	L2	L3	Status
			(%)			
3	150	7	1.96	1.66	1.62	Within
5	250	7	0.32	0.13	0.18	Within
7	350	7	0.03	0.05	0.02	Within
9	450	7	0.02	0.06	0.03	Within
11	550	3.5	0	0	0	Within
THD	—	**8**	**1.99**	**1.66**	**1.63**	**Within**

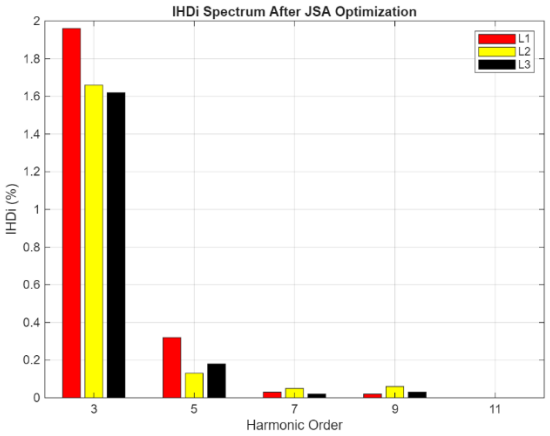

Fig 9. IHDi Spectrum Optimized by JSA

C. COMPARATIVE PERFORMANCE ANALYSIS OF HARMONIC MITIGATION

Based on Fig 10., the three-dimensional cylindrical visualization presents a comparative analysis of Total Harmonic Distortion (THD) across three phases (L1, L2, and L3) under four conditions: the IEEE standard limit, measured values, conventional calculation results, and optimization using the Jellyfish Search Algorithm (JSA). The IEEE limit is uniformly set at 8% for all phases and serves as the regulatory benchmark. The measured THD values significantly exceed this threshold, reaching 23.55% in L1, 18.67% in L2, and 24.72% in L3, as indicated by the tallest cylinders with dominant red–orange gradients, reflecting severe harmonic distortion and poor power quality. The implementation of the conventional method substantially improves system performance, lowering THD to 3.25%, 3.16%, and 3.36% for L1, L2, and L3, respectively, thereby achieving compliance with the IEEE standard. A more pronounced improvement is observed with the JSA-based optimization, which yields THD values of 1.99% (L1), 1.66% (L2), and 1.63% (L3). These results are represented by the shortest cylinders with deep blue coloration, indicating superior harmonic mitigation capability. Overall, the 3D visualization demonstrates that while the conventional approach effectively ensures regulatory compliance, the JSA-based optimization provides more optimal and consistent harmonic mitigation performance across all phases, aligning with the objective of advanced passive filter design for enhanced power quality.

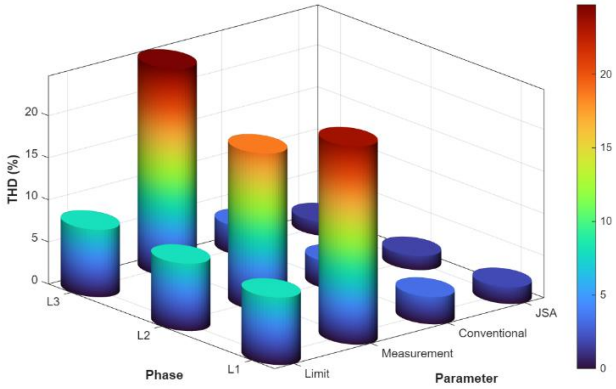

Fig 10. 3D THD Performance Comparison

IV. CONCLUSION

The design and evaluation of the C-Type passive filter demonstrate that harmonic mitigation in medium-voltage industrial distribution systems can be significantly improved through parameter optimization. While the conventional analytical method is capable of reducing Total Harmonic Distortion (THD) to comply with the IEEE 519, it does not fully account for system-specific harmonic characteristics, resulting in suboptimal suppression of dominant components such as the 3rd harmonic. In contrast, the Jellyfish Search Algorithm (JSA) provides an adaptive optimization framework that enables more accurate tuning of filter parameters according to the actual system conditions. This leads to more effective harmonic attenuation, improved consistency across

phases, and enhanced overall power quality. The obtained results indicate that no significant harmonic amplification is observed at non-targeted frequencies, suggesting stable filter operation within the studied conditions. Therefore, the proposed JSA-based C-Type filter design offers a robust and practical approach for harmonic mitigation, with strong potential for application in industrial power systems requiring reliable and optimized power quality performance.

REFERENCES

[1] K. Srilakshmi *et al.*, "Development of renewable energy fed three-level hybrid active filter for EV charging station load using Jaya grey wolf optimization," *Sci. Rep.*, vol. 14, no. 1, p. 4429, 2024, doi: 10.1038/s41598-024-54550-7.

[2] M. Upanya, S. Anushree, M. Masood, G. N. Deekshitha, and K. P. N. Kumara, "Harmonic Mitigation Using Active and Passive Filters," in *2025 International Conference on Sustainable Energy Technologies and Computational Intelligence (SETCOM)*, 2025, pp. 1–6. doi: 10.1109/SETCOM64758.2025.10932454.

[3] A. Refaie Ali, M. R. Islam, S. Islam, Fatima-Tuz-Zohura, and I. Nurhidayat, "Design a passive filter in combination with SAPF to improve the power quality of the solar hybrid micro-grid system and combustion engines," *Sustain. Energy Res.*, vol. 12, no. 1, 2025, doi: 10.1186/s40807-025-00181-z.

[4] M. Z. Bin Rozman and R. M. Idris, "Comparison of Active Power Filter and Passive Power Filter in Harmonic Mitigation in Power System Network," *Elektr. J. Electr. Eng.*, vol. 24, no. 3, pp. 284–290, 2025, doi: 10.11113/elektrika.v24n3.718.

[5] H. Aprillia, A. Rifa'i, and Y. T. K. Priyanto, "Modeling a PI-GWO controlled shunt active power filter in 14-bus IEEE system," *AIP Conf. Proc.*, vol. 3272, no. 1, p. 30001, 2025, doi: 10.1063/5.0282745.

[6] H. Zhang *et al.*, "Harmonic control method for multiple driving cycles of EMU based on improved C-type filter," *J. Eng. Appl. Sci.*, vol. 70, no. 1, pp. 1–17, 2023, doi: 10.1186/s44147-023-00321-6.

[7] M. I. Malik and E. Ihsanto, "Design and Simulation High Pass Filter Second Order and C-Type Filter for Reducing Harmonics as Power Quality Repair Effort in the Automotive Industry," *J. Integr. Adv. Eng.*, vol. 3, no. 1, pp. 23–36, 2023, doi: 10.51662/jiae.v3i1.79.

[8] M. I. Malik, Y. M. Hamdani, R. Nurdiansyah, L. Faridah, and Nurmela, "Hybrid Double-Tuned and High-Pass Filter for Harmonic Mitigation in Inverter HVAC Systems ," *ELECTRON J. Ilm. Tek. Elektro*, vol. 6, no. 2 SE-Articles, pp. 139 – 152, Nov. 2025, doi: 10.33019/electron.v6i2.387.

[9] M. I. Malik, Y. M. Hamdani, and Yanti, "Optimization Design of Single-Tuned Passive Filter Using Particle Swarm Optimization Algorithm in Industry," *J. Energy Electr. Eng.*, vol. 6, no. 2, pp. 137–144, 2025, doi: https://doi.org/10.37058/jeee.v6i2.14644.

[10] M. D. Faraby *et al.*, "Whale Optimization Algorithm to Optimal Placement and Size of Single Tuned Filter in PT. Semen Tonasa," in *2025 IEEE Power Electronics Society International Decentralized Energy Access Symposium (IDEAS)*, 2025, pp. 1–6. doi: 10.1109/IDEAS62193.2025.11157292.

[11] F. Sanchez, A. R. Lopez, J. M. Sosa, M. J. Villaseñor-Aguilar, S. E. D. Leon-Aldaco, and J. A. Alquicira, "Design of Passive Filters for Power Inverters Using a Genetic Algorithm," in *2025 5th International Conference on Electrical, Computer, Communications and Mechatronics Engineering (ICECCME)*, 2025, pp. 1–6. doi: 10.1109/ICECCME64568.2025.11277465.

[12] D. Peng, K. Xie, and M. Liu, "Application of Gray Wolf Particle Filter Algorithm Based on Golden Section in Wireless Sensor Network Mobile Target Tracking," *Electronics*, vol. 13, no. 13, 2024, doi: 10.3390/electronics13132440.

[13] W. Jiang, Z. Liu, Y. Wang, Y. Lin, Y. Li, and F. Bi, "Enhancing jamming source tracking capability via adaptive grey wolf optimization mechanism for passive radar network," *Signal Processing*, vol. 235, p. 110026, 2025, doi: https://doi.org/10.1016/j.sigpro.2025.110026.

[14] N. Li, W. Xu, Q. Zeng, Y. Ren, W. Ma, and K. Tan, "A hybrid WOA-CNN-BiLSTM framework with enhanced accuracy for low-voltage shunt capacitor remaining life prediction in power systems," *Energy*, vol. 326, p. 136183, 2025, doi: https://doi.org/10.1016/j.energy.2025.136183.

[15] U. J. Aniekwensi, D. Basu, and J. Bausch, "Data-driven machine learning model estimates efficiency gains from passive filters under

variable loads," *Energy AI*, vol. 22, p. 100631, 2025, doi: https://doi.org/10.1016/j.egyai.2025.100631.

[16] A. Khare, G. M. Kakandikar, and O. K. Kulkarni, "An Insight Review on Jellyfish Optimization Algorithm and Its Application in Engineering," *Rev. Comput. Eng. Stud.*, vol. 9, no. 1, pp. 31–40, 2022, doi: 10.18280/rces.090103.

[17] J. S. Chou and A. Molla, "Recent advances in use of bio-inspired jellyfish search algorithm for solving optimization problems," *Sci. Rep.*, vol. 12, no. 1, pp. 1–23, 2022, doi: 10.1038/s41598-022-23121-z.

[18] G. Manita and A. Zermani, "A modified jellyfish search optimizer with orthogonal learning strategy," *Procedia Comput. Sci.*, vol. 192, pp. 697–708, 2021, doi: 10.1016/j.procs.2021.08.072.

[19] J. S. Chou, N. Q. Nguyen, and K. Srinivasan, "Forecasting Regional Energy Consumption via Jellyfish Search-Optimized Convolutional-Based Deep Learning," *Int. J. Energy Res.*, vol. 2023, 2023, doi: 10.1155/2023/3056688.

[20] A. A. El-ela, R. El-sehiemy, S. M. Allam, and A. A. Mubarak, "Optimal sizing and siting of single tunned passive filter based on jellyfish algorithm," *Energy Technol. Environ.*, vol. 2, no. April, pp. 15–28, 2024, doi: 10.58567/ete.

[21] V. Chenna and H. Hashemi, "Algorithmic Design of Nonintuitive on-Chip Multilayered Passive Networks," in *2025 IEEE/MTT-S International Microwave Symposium - IMS 2025*, 2025, pp. 918–921. doi: 10.1109/IMS40360.2025.11103811.

[22] A. M. Alam, M. Kurum, and A. C. Gurbuz, "Deep Learning-Based High-Resolution Time-Frequency Domain RFI Suppression in Passive Systems," in *IGARSS 2025 - 2025 IEEE International Geoscience and Remote Sensing Symposium*, 2025, pp. 404–408. doi: 10.1109/IGARSS55030.2025.11244022.

[23] J. C. Das, "Passive Filters," in *Power System Harmonics and Passive Filter Designs*, IEEE, 2015, pp. 685–743. doi: 10.1002/9781118887059.ch15.

[24] R. Tamaskani, M. Khodsuz, and M. Yazdani-asrami, "Optimal Design of C-Type Filter in Harmonics Polluted Distribution Systems," *Energies*, vol. 15, no. 4, 2022, doi: 10.3390/en15041587.

[25] A. G. Lange and G. Redlarski, "Selection of C-type filters for reactive power compensation and filtration of higher harmonics injected into the transmission system by arc furnaces," *Energies*, vol. 13, no. 9, 2020, doi: 10.3390/en13092330.

[26] H. Ali I. Gony, G. Izat Rashed, A. Badjan, A. O. M. Bahageel, and H. I. Shaheen, "Advanced Harmonic Mitigation in Photovoltaic Grid-Connected Systems: Jellyfish Search Optimization Approach," *Elektr. J. Electr. Eng.*, vol. 23, no. 3, pp. 6–18, 2024, doi: 10.11113/elektrika.v23n3.544.

[27] J. Ranga *et al.*, "Optimization of Distributed Generation in Radial Distribution Network for Active Power Loss Minimization using Jellyfish Search Optimizer Algorithm," *Int. J. Electr. Comput. Eng. Syst.*, vol. 15, no. 3, pp. 215–223, 2024, doi: 10.32985/ijeces.15.3.1.

[28] H. C. Trong, T. T. Nguyen, and T. T. Nguyen, "Jellyfish search algorithm for economic load dispatch under the considerations of prohibited operation zones, load demand variations, and renewable energy sources," *IAES Int. J. Artif. Intell.*, vol. 13, no. 1, pp. 74–81, 2024, doi: 10.11591/ijai.v13.i1.pp74-81.

[29] P. T. Ha, B. H. Dinh, T. M. Phan, and T. T. Nguyen, "Jellyfish search algorithm for optimization operation of hybrid pumped storage-wind-thermal-solar photovoltaic systems," *Heliyon*, vol. 10, no. 7, p. e29339, 2024, doi: 10.1016/j.heliyon.2024.e29339.

AUTHORS BIOGRAPHY AND CONTRIBUTIONS

Mochamad Irlan Malik, is a Lecturer and Researcher in the Department of Electrical Engineering at Universitas Siliwangi, Indonesia. He received his Bachelor's degree in Electrical Engineering from Universitas Gunadarma in 2013 and his Master's degree in Electrical Engineering from Universitas Mercu Buana in 2022. His research interests include signal and systems, power quality optimization, and wireless power transfer.

Nurmela, is a Lecturer and Researcher in the Department of Electrical Engineering at Universitas Siliwangi. She obtained her Bachelor's degree in Electrical Engineering from Universitas Siliwangi in 2018 and her Master's degree in Electrical

Engineering from Institut Teknologi Bandung in 2022. She is currently pursuing her doctoral studies at Institut Teknologi Bandung. She has professional experience in power system analysis and has been actively involved in teaching and community service activities. Her research interests include power systems, renewable energy, and smart grid technologies.

Boy Ihsan, is a Lecturer and Researcher in the Department of Electrical Engineering at Universitas Riau, Indonesia. He obtained his Bachelor's degree in Electrical Engineering from Universitas Riau in 2017 and his Master's degree in Electrical Engineering from Institut Teknologi Bandung in 2022. His research interests include power systems, renewable energy, net-zero emissions, artificial intelligence, and energy storage.

Nadya Glaudira, is a Lecturer and Researcher in the Department of Electrical Engineering at Universitas Siliwangi, Indonesia. She received her Applied Bachelor's degree in Telecommunication Engineering from Politeknik Negeri Bandung in 2017 and her Master's degree in Electrical Engineering from Institut Teknologi Bandung in 2023. Her research focuses on telecommunications engineering, particularly in the design and analysis of MIMO antenna systems.

Mulyana, recently completed his Master's degree in Electrical Engineering at Universitas Islam Sultan Agung, Semarang, in 2026. He received his Bachelor's degree in Mechanical Engineering from STT YBS Internasional in 2022. His academic background reflects an interdisciplinary focus spanning mechanical and electrical engineering. His research interests include mechatronics and metaheuristic optimization.